Vol. 25, No. 3(2026) Poly26787

Revista Mexicana de Ingeniería Química

Rheological behavior and integrated modeling of polymer solutions under reservoir-representative conditions

Comportamiento reológico y modelado integrado de soluciones poliméricas bajo condiciones representativas de yacimiento

E. Rodríguez-Sánchez[2], A. D. Miranda-Olvera[1]*, T. Roldán-Carrillo[1], M.Á. De la Rosa-Guzmán[2], P. Olguin-Lora[1]

[1] Instituto Mexicano del Petróleo. Eje Central Lázaro Cárdenas Norte 152, 07750, GAM, CDMX, México
[2] Instituto Politécnico Nacional. ESIQIE, Zacatenco, 07738 CDMX, México

Received: February 19, 2026; Accepted: June 1, 2026

Abstract

This study evaluates the rheological behavior of three polymers widely used in Enhanced Oil Recovery (EOR) applications: xanthan gum (XG), partially hydrolyzed polyacrylamide (HPAM), and sulfonated polyacrylamide (FLOPAAM). The polymers were tested under reservoir-representative conditions, including temperatures up to 80 °C, pressures up to 6000 psi, and synthetic brine diluted to 10% of the reservoir salinity, to assess their apparent viscosity, shear response, and rheological stability under demanding operating environments. Apparent viscosity–shear rate measurements confirmed that all polymer solutions exhibited pronounced shear-thinning behavior. XG demonstrated elevated consistency index values and high thermal stability under the studied brine conditions. FLOPAAM exhibited enhanced rheological stability under combined shear-rate and pressure effects, consistent with the presence of sulfonate functional groups. HPAM maintained acceptable rheological performance at higher concentrations but displayed greater sensitivity to temperature and pressure variations. The experimental data were accurately described using the Ostwald–de Waele power-law model ($R^2 > 0.98$), selected for its robustness and suitability for comparative analysis. Based on this framework, an integrated apparent viscosity framework was developed based on well-established rheological correlations in which shear-rate dependence follows the power-law formulation, concentration and temperature effects are incorporated through the consistency index, and pressure effects are introduced independently via an inverse Barus-type relation. This hierarchical approach avoids overparameterization while preserving physical interpretability. The proposed framework provides a physically consistent approach for describing and interpolating polymer rheology under reservoir-relevant conditions and supports rational polymer selection within the experimental domain investigated.

Keywords: Enhanced Oil Recovery; Polymer Flooding; Rheology; Apparent Viscosity; Xanthan Gum; HPAM; FLOPAAM.

Resumen

Este estudio evalúa el comportamiento reológico de tres polímeros ampliamente utilizados en aplicaciones de Recuperación Mejorada de Petróleo (EOR): goma xantana (XG), poliacrilamida parcialmente hidrolizada (HPAM) y poliacrilamida sulfonada (FLOPAAM). Los polímeros fueron evaluados bajo condiciones representativas de yacimiento, incluyendo temperaturas de hasta 80 °C, presiones de hasta 6000 psi y salmuera sintética diluida al 10 % de la salinidad del yacimiento, con el fin de analizar su viscosidad aparente, respuesta al esfuerzo cortante y estabilidad reológica en entornos operativos demandantes. Las mediciones de viscosidad aparente en función de la velocidad de corte confirmaron que todas las soluciones poliméricas exhiben un comportamiento marcadamente pseudoplástico. La goma xantana (XG) mostró valores elevados del índice de consistencia y alta estabilidad térmica bajo las condiciones de salmuera estudiadas. FLOPAAM presentó una mayor estabilidad reológica bajo efectos combinados de velocidad de corte y presión, en concordancia con la presencia de grupos funcionales sulfonato. HPAM mantuvo un desempeño reológico aceptable a concentraciones elevadas, aunque evidenció una mayor sensibilidad frente a variaciones de temperatura y presión. Los datos experimentales fueron descritos adecuadamente mediante el modelo de ley de potencia de Ostwald–de Waele ($R^2 > 0.98$), seleccionado por su robustez y pertinencia para el análisis comparativo. Con base en este enfoque, se desarrolló un marco integrado de viscosidad aparente sustentado en correlaciones reológicas bien establecidas, en el cual la dependencia con la velocidad de corte se describe mediante la formulación de ley de potencia, mientras que los efectos de concentración y temperatura se incorporan a través del índice de consistencia, y los efectos de presión se introducen de manera independiente mediante una relación tipo Barus inversa. Este enfoque jerárquico evita la sobreparametrización y preserva la interpretabilidad física de los parámetros. El marco propuesto proporciona un enfoque físicamente consistente para describir e interpolar la reología de soluciones poliméricas bajo condiciones relevantes de yacimiento y respalda la selección racional de polímeros dentro del dominio experimental investigado.

Palabras clave: Recuperación Mejorada de Petróleo; Inyección de Polímeros; Reología; Viscosidad Aparente; Goma Xantana, HPAM, FLOPAAM.

* *Corresponding author. E-mail*: admiranda@imp.mx ;
https://doi.org/10.24275/rmiq/Poly26787
ISSN:1665-2738, *issn-e*: 2395-8472

1 Introduction

The exploitation of hydrocarbons continues to play a central role in the global energy matrix. However, the progressive depletion of conventional reservoirs has driven the oil industry toward the development of more complex resources, particularly heavy and extra-heavy oils, which account for more than 70% of worldwide hydrocarbon reserves (Gomaa *et al*., 2024). These crude oils are characterized by high apparent viscosity, low API gravity, and unfavorable flow properties, which significantly reduce their mobility and limit production efficiency under primary and secondary recovery methods.

In this context, Enhanced Oil Recovery (EOR) techniques have gained increasing relevance to improve sweep efficiency and mobilize the remaining oil within the reservoir. Among the available EOR methods, chemical approaches—particularly polymer flooding—have demonstrated high effectiveness in heterogeneous formations and heavy oil systems by increasing the apparent viscosity of the displacing phase and improving the mobility ratio (Rock *et al*., 2020; Chen *et al*., 2013; Tahir *et al*., 2020).

The success of polymer flooding is strongly dependent on the appropriate selection of the polymeric agent, which must retain its rheological functionality under reservoir conditions. The most employed polymers include xanthan gum (XG), a biopolymer known for its good tolerance to salinity and moderate thermal stability; partially hydrolyzed polyacrylamide (HPAM), a synthetic polymer widely used due to its favorable viscosity performance and economic advantages; and sulfonated polyacrylamides, such as FLOPAAM AN-113, whose sulfonate groups enhance resistance to thermal and saline degradation. Figure 1 shows representative chemical structures of the evaluated polymers.

These polymers typically exhibit shear-thinning and viscoelastic behavior, which facilitates their transport through porous media across a wide range of shear conditions and enhances their effectiveness in mobility control during EOR operations. Similar pseudoplastic behavior and temperature-dependent variations in rheological parameters have been reported for xanthan gum-based systems modeled using power-law and Arrhenius-type approaches (Soto-Caballero *et al*., 2016). In addition, several studies have reported the ability of certain polymers to induce selective permeability reduction, preferentially reducing water permeability while preserving oil permeability (Gbadamosi *et al*., 2019). Nevertheless, polymer stability and rheological functionality may deteriorate under harsh reservoir conditions, which are frequently encountered in mature fields (Castro García *et al*., 2020; Skauge *et al*., 2022).

Despite significant advances in the rheological characterization of polymers for EOR applications, many studies remain focused on the influence of isolated operational variables, such as temperature or salinity, without addressing their combined effects under realistic reservoir conditions. For example, Saeed *et al*. (2023) investigated the stability of HPAM and sulfonated derivatives in saline environments; however, comprehensive comparative analyses involving multiple polymers under simultaneous temperature, pressure, and salinity conditions remain relatively scarce. Moreover, there is a lack of rheological models capable of integrating the coupled effects of shear rate, temperature, and pressure in a physically consistent framework suitable for injection design and performance prediction (Saeed & Jadhawar, 2023).

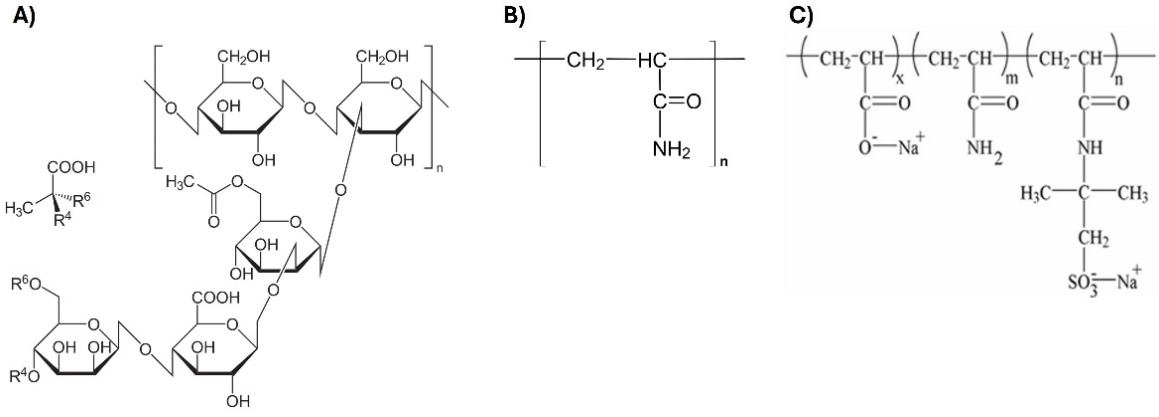

Fig. 1 Representative chemical structures of the evaluated polymers: (A) xanthan gum (XG); (B) partially hydrolyzed polyacrylamide (HPAM); (C) sulfonated polyacrylamide (FLOPAAM AN-113).

In this study, a comparative rheological evaluation of three commercial polymers—XG, HPAM, and FLOPAAM AN-113—is presented under reservoir-representative conditions, including pressures up to 6000 psi, temperatures up to 80 °C, and an original connate-water salinity of approximately 67,000 ppm TDS. Polymer solutions were prepared in synthetic brine diluted to 10% of the original salinity, consistent with low-salinity water injection (LSWI) strategies aimed at improving oil recovery efficiency and modifying physicochemical interactions under reservoir conditions (Carmona-Pérez *et al.*, 2026). Apparent viscosity–shear rate curves were obtained at different polymer concentrations using a high-precision rheometer equipped with temperature and pressure control. The experimental data were analyzed using the Ostwald–de Waele power-law model to characterize shear-dependent behavior and to develop an integrated and physically consistent rheological framework that combines established correlations to incorporate the coupled effects of shear rate, temperature, and pressure.

The objective of this work is to address existing gaps in the comprehensive rheological characterization of polymers under complex operating conditions. The results provide practical criteria for polymer selection and formulation optimization in EOR processes, particularly in mature and operationally demanding reservoirs, and contribute to the rational design of thermomechanically stable polymer systems tailored to specific reservoir environments.

2 Materials and methods

2.1 Evaluated Polymers

Three polymers commonly employed in Enhanced Oil Recovery (EOR) applications were evaluated: xanthan gum (XG), partially hydrolyzed polyacrylamide (HPAM), and sulfonated polyacrylamide (FLOPAAM AN-113). These materials were selected based on their distinct chemical structures and their documented tolerance to critical reservoir conditions, including temperature, salinity, and pressure.

XG was supplied by COINA and has an average molecular weight typically on the order of 10^6-10^7 Da, consistent with high-molecular-weight biopolymers used in EOR applications. HPAM was purchased from Ingeniería Liquid Technologies and is characterized by a hydrolysis degree of approximately 30% and a high molecular weight commonly observed for partially hydrolyzed polyacrylamides in the 10^6–10^7 Da range. FLOPAAM AN-113, provided by SNF Floerger®, is a copolymer of acrylamide and 2-acrylamido-2-methylpropane sulfonic acid (AMPS) with high molecular weight; commercial sulfonated polyacrylamides of this class typically range from less than 2×10^6 Da up to about 2.2×10^7 Da. Representative chemical structures of the evaluated polymers are presented in Figure 1.

2.2 Preparation of Polymer Solutions

Polymer solutions were prepared at concentrations ranging from 800 to 5000 ppm. This concentration range was selected based on literature reports indicating its technical relevance in EOR operations, as it provides sufficient viscosity enhancement while minimizing adverse effects on injectivity and avoiding undesirable phenomena such as gelation or excessive aggregation (Seright, 2017; Zaitoun & Kohler, 1988a).

Synthetic brine (SB) was used as the solvent, formulated based on the ionic composition and total dissolved solids of the reservoir connate water, whose original salinity was approximately 67,000 ppm. In this study, the brine was diluted to 10% of the original salinity, corresponding to an effective salinity of approximately 6,700 ppm, in accordance with Low-Salinity Water Injection (LSWI) strategies aimed at improving oil recovery through controlled ionic strength. This dilution allows the assessment of polymer rheological performance under salinity levels representative of field-scale EOR applications.

The chemical composition of the 10% synthetic brine (10% SB) is summarized in Table 1 and was defined based on Atomic Absorption Spectroscopy (AAS) analysis of the reservoir brine to quantify dissolved metallic species.

The selected salinity level represents a compromise between reservoir representativeness and operational conditions commonly employed in low-salinity water injection (LSWI) strategies. Although higher salinity levels are typical of many reservoirs, the present study focuses on conditions where salinity is intentionally reduced to enhance polymer performance and oil recovery efficiency.

For each solution, the polymer was gradually added to the total volume of 10% synthetic brine under constant stirring at 500 rpm for 2 h using a magnetic stirrer with temperature control. The solutions were subsequently allowed to rest for 24 h at ambient temperature (25 °C) to ensure complete polymer hydration and structural equilibrium prior to rheological testing. The final pH of the solutions ranged between 6.5 and 7.2.

2.3 Rheological analysis

Rheological measurements were conducted using an Anton Paar® MCR 502 rheometer (SN 812079) equipped with a concentric cylinder geometry (CC27, SN 30287) and a Peltier temperature control system (PTD 200, SN 81217359). Data acquisition and processing were performed using RheoCompass® software.

Table 1. Chemical composition of the synthetic brine (SB) and diluted brine (10% SB).

No	Compound	Formula	SB (mg/L)	10% SB (mg/L)
1	Sodium chloride	NaCl	66859.5	6685.95
2	Magnesium chloride hexahydrate	$MgCl_2{\cdot}6H_2O$	4358.2	435.82
3	Sodium bicarbonate	$NaHCO_3$	514.3	51.43
4	Calcium chloride dihydrate	$CaCl_2{\cdot}2H_2O$	27988.8	2798.88
5	Iron (II) chloride tetrahydrate	$FeCl_2{\cdot}4H_2O$	0.4	0.04
6	Manganese (II) sulfate monohydrate	$MnSO_4{\cdot}H_2O$	1.2	0.12
7	Strontium chloride hexahydrate	$SrCl_2{\cdot}6H_2O$	1738.1	173.81
8	Potassium chloride	KCl	2637.3	263.73
9	Barium chloride	$BaCl_2$	1.5	0.15
10	Sodium sulfate	Na_2SO_4	150.8	15.08

SB formulation derived from reservoir connate water composition.

Experiments were carried out over a shear rate range of 1 to 100 s^{-1} and at controlled temperatures between 20 and 80 °C, representative of reservoir thermal conditions. Each test was performed in triplicate to ensure reproducibility and minimize experimental uncertainty.

To simulate downhole pressure conditions, a high-pressure module was coupled to the rheometer. The pressurization system consisted of a nitrogen-fed cylinder with a maximum operating pressure of 6000 psi, inlet and outlet pressure control valves, a pressure transducer for continuous real-time monitoring, and a compressor–cooler assembly to maintain stable operating conditions. This configuration enabled the acquisition of apparent viscosity–shear rate curves under simultaneous temperature and pressure control.

All rheological data and modeling equations were formulated using SI units. However, for clarity and consistency with reservoir engineering practice, temperatures are reported in °C and pressures in psi in figures and tables. Apparent viscosity is denoted by η_{app} and expressed in mPa·s. Shear stress is denoted by τ (Pa), shear rate by $\dot{\gamma}$ (s^{-1}), consistency index by K (mPa·s^n), and flow behavior index by n (dimensionless).

In the Barus-type pressure model, the coefficient α (Pa^{-1} or psi^{-1}) quantifies pressure sensitivity. Negative values of α indicate compressive behavior of the polymer solution, resulting in a decrease of apparent viscosity with increasing pressure.

2.4 Data Processing and Visualization Using Power BI

Experimental data were processed and visualized using Power BI as a dynamic and interactive analysis tool. The evaluated variables included shear rate, apparent viscosity, polymer concentration, temperature, pressure, polymer type (XG, HPAM, FLOPAAM), and solvent composition (10% synthetic brine).

Interactive dashboards were developed incorporating scatter plots (apparent viscosity versus shear rate) and line charts (apparent viscosity versus temperature and concentration), along with filters for polymer type and operating conditions. This approach facilitated identification of rheological trends, confirmation of shear-thinning behavior, and evaluation of polymer stability under critical reservoir-representative conditions.

3 Results and discussion

The rheological behavior of xanthan gum (XG), partially hydrolyzed polyacrylamide (HPAM), and sulfonated polyacrylamide (FLOPAAM) were evaluated under controlled temperature, pressure, and salinity conditions, including diluted synthetic brine representative of low-salinity water injection (LSWI) strategies. In all cases, pronounced shear-thinning behavior was observed, as indicated by the systematic decrease in apparent viscosity (η_{app}) with increasing shear rate ($\dot{\gamma}$). This behavior is characteristic of polymer solutions employed for mobility control and is consistent with trends widely reported in the literature (Tapias Hernández *et al.*, 2018; Zaitoun & Kohler, 1988b).

3.1 Effect of Temperature and Concentration on XG Rheology

Xanthan gum (XG) solutions exhibited a pronounced shear-thinning behavior over the full range of concentrations and temperatures investigated, as evidenced by the progressive decrease in apparent viscosity with increasing shear rate (Figure 2). This non-Newtonian response is characteristic of semi-rigid biopolymers and confirms the suitability of the power-law model to represent the experimental flow curves.

At a polymer concentration of 1000 ppm and 80 °C, the apparent viscosity in 10% synthetic brine was approximately 7.4 mPa·s at a shear rate of 4.6 s^{-1}.

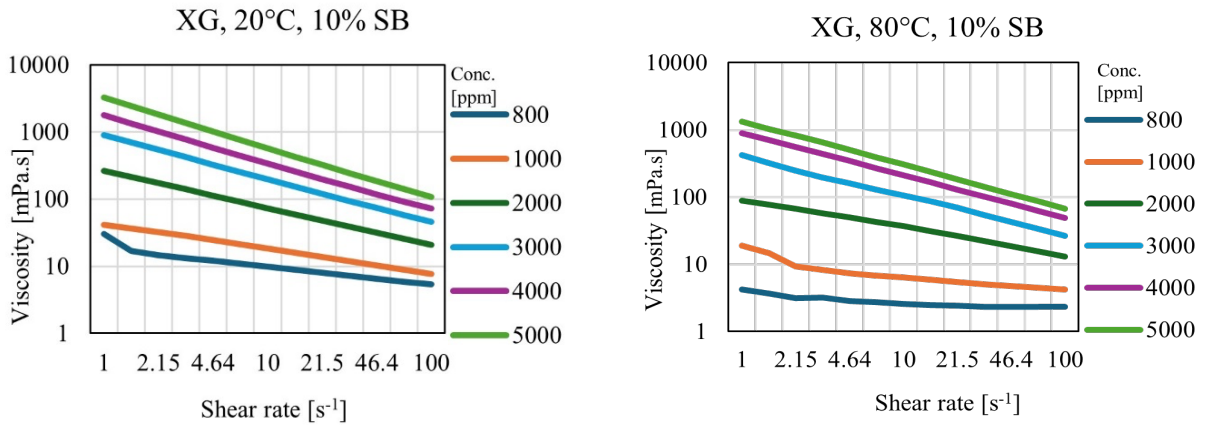

Fig. 2 Apparent viscosity-shear rate curves for xanthan gum (XG) solutions in 10% synthetic brine.

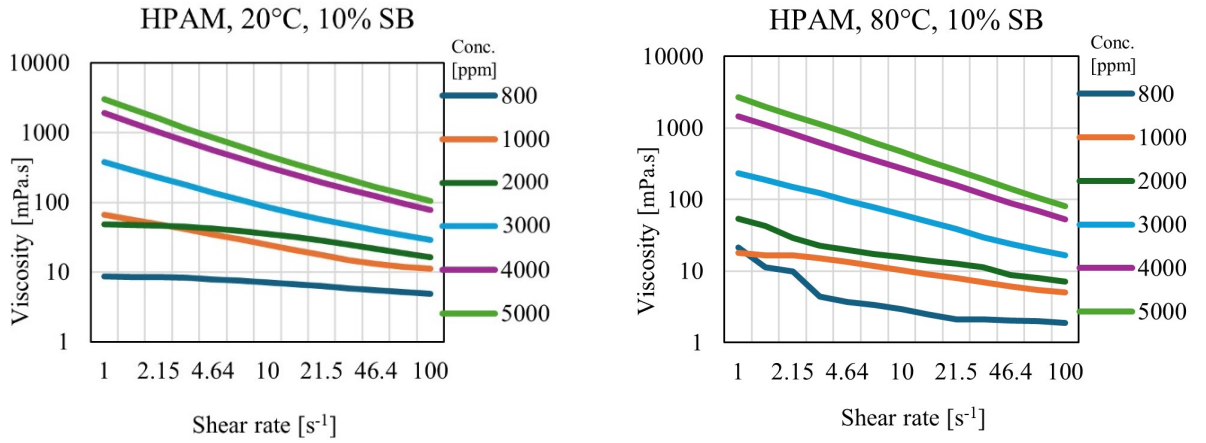

Fig. 3 Apparent viscosity-shear rate curves for HPAM solutions in 10% synthetic brine.

In contrast, at 5000 ppm, the apparent viscosity exceeded 500 mPa·s at the same shear rate, representing an increase of nearly two orders of magnitude. This increase is reflected in the consistency index, which rises from approximately 0.01 to 1.34 mPa·s^n over the evaluated concentration range (Table 2), indicating a significant enhancement in network strength. This pronounced concentration effect is associated with enhanced intermolecular interactions and network structuring, which is reflected in higher consistency index values.

At polymer concentrations below approximately 2000 ppm, reduced apparent viscosity values were observed. This behavior is consistent with partial electrostatic screening under the ionic strength conditions of the diluted brine (10% SB). At higher concentrations, intermolecular associations and transient network structures likely mitigated viscosity reductions.

Increasing temperature resulted in a systematic reduction of apparent viscosity, which can be attributed to the weakening of intermolecular cohesive forces and partial disruption of the polymeric network. Despite this thermal thinning effect, XG maintained a functional apparent viscosity under combined salinity and temperature conditions, confirming its suitability for moderate-temperature reservoir environments. These trends are consistently captured by the proposed concentration–temperature dependence of the consistency index, reinforcing the physical relevance of the developed rheological framework.

3.2 *Effect of Temperature and Concentration on HPAM Rheology*

Partially Hydrolyzed Polyacrylamide (HPAM) solutions exhibited pronounced shear-thinning behavior under all tested conditions, characterized by a systematic decrease in apparent viscosity with increasing shear rate (Figure 3). This response is consistent with the expected rheological behavior of flexible polymer chains in solutions and confirms the applicability of the power-law model as a base description of the experimental flow curves.

At a polymer concentration of 1000 ppm, 80 °C, and in 10% synthetic brine, the apparent viscosity was approximately 10 mPa·s at a shear rate of 10 s^{-1}. In contrast, at 5000 ppm, apparent viscosity values

approaching 2000 mPa·s were obtained at the lowest shear rates (~1 s^{-1}), confirming the strong dependence of the rheological response on polymer concentration. This effect is associated with increased chain overlap and entanglement, leading to higher consistency index values as concentration increases.

HPAM displayed pronounced temperature sensitivity, particularly at low polymer concentrations. At elevated temperature (80 °C), apparent viscosity decreased significantly due to enhanced molecular mobility, weakening of stabilizing intermolecular interactions including hydrogen bonding and electrostatic forces. Additionally, the ionic strength of the diluted synthetic brine (10% SB) likely contributed to viscosity reduction through partial electrostatic screening and contraction of polymer chains, which limited chain expansion and reduced the hydrodynamic volume of the macromolecules.

This behavior is consistent with the decrease in the consistency index K and the increase in the flow behavior index n at higher temperatures, indicating reduced structural resistance and a transition toward less pseudoplastic behavior (Table 2).

At higher concentrations (3000–5000 ppm), HPAM exhibited partial rheological stability; however, its performance deteriorated under the combined effects of elevated temperature and the ionic strength conditions of the diluted synthetic brine (10% SB). In dilute systems (<1000 ppm), the polymer exhibited reduced shear dependence at high shear rates, which may limit its applicability in high-flow-rate environments where apparent viscosity losses become critical.

Overall, HPAM remains a feasible polymer for moderate reservoir conditions; however, its rheological performance is highly sensitive to temperature and concentration. These trends are consistently reflected in the proposed concentration–temperature dependence of the consistency index, emphasizing the importance of concentration optimization and appropriate brine chemistry selection for effective and economically viable EOR applications.

3.3 Effect of Temperature and Concentration on FLOPAAM Rheology

Sulfonated Polyacrylamide (FLOPAAM) solutions exhibited consistent shear-thinning behavior across the evaluated temperature and concentration ranges, with notable retention of apparent viscosity at low shear rates (Figure 4). At 5000 ppm and 20 °C, the apparent viscosity exceeded 90 mPa·s at a shear rate of 4.6 s^{-1}. Even at 80 °C, viscosity values remained above 40 mPa·s under identical shear conditions, indicating enhanced thermal stability at high polymer concentrations. This behavior is consistent with the electrolyte tolerance commonly reported for sulfonated polyacrylamides (Ghalamizade *et al.*, 2025).

At lower concentrations (800–3000 ppm), the initial apparent viscosity was significantly lower and decreased rapidly with increasing shear rate and temperature. This behavior suggests that a critical polymer chain density is required to establish a cohesive structural network capable of resisting hydrodynamic deformation, particularly under thermally and mechanically demanding conditions.

Table 2. Ostwald-de Waele model parameters (T = 80 °C) for polymer solutions in 10% synthetic brine.

Polymer solution	Concentration (ppm)	K (mPa.s^n)	n	R^2
XG in 10% SB	5000	1.3404	0.4026	0.9894
	4000	0.8471	0.4237	0.9938
	3000	0.4347	0.377	0.9937
	2000	0.0951	0.5898	0.9973
	1000	0.0118	0.7507	0.9999
HPAM in 10% SB	5000	2.0705	0.3713	0.986
	4000	1.1824	0.3951	0.9831
	3000	0.1658	0.3467	0.9666
	2000	0.1031	0.5652	0.9678
	1000	0.0181	0.7959	0.9707
FLOPAAM in 10% SB	5000	0.0518	0.8236	0.9842
	4000	0.0296	0.879	0.9892
	3000	0.0159	0.8332	0.9989
	2000	0.0084	0.8232	0.9993
	1000	0.0033	0.8355	0.9948

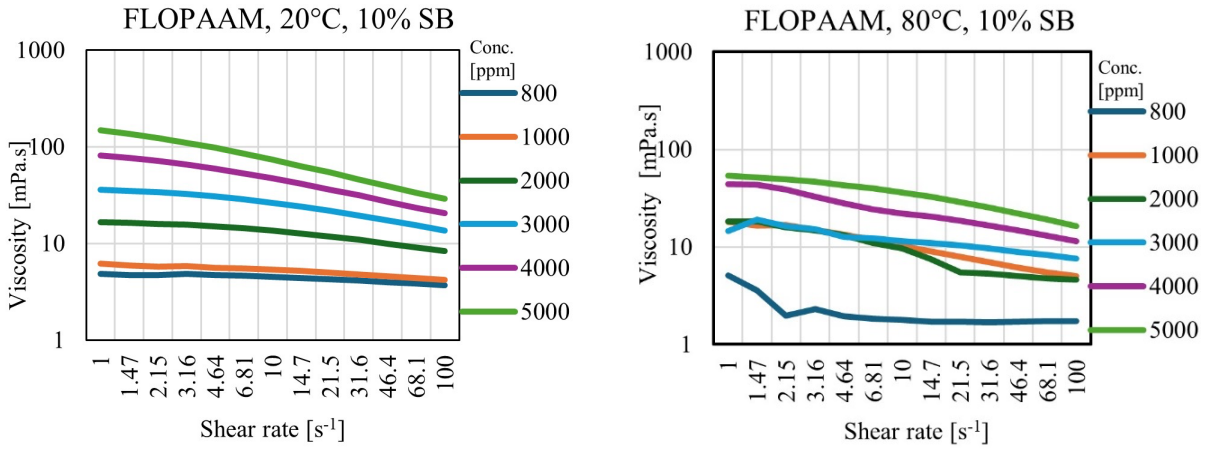

Fig. 4 Apparent viscosity-shear rate curves for FLOPAAM solutions in 10% synthetic brine.

Although FLOPAAM exhibited lower apparent viscosity values than XG at equivalent concentrations, its viscosity decay with shear rate was less pronounced. Moreover, the shape of the viscosity-shear rate curves showed reduced sensitivity to temperature (20–80 °C), suggesting a more temperature-robust shear response under the studied brine conditions. These results reinforce the relevance of concentration as a key design parameter while highlighting FLOPAAM as a polymer with a more predictable flow behavior across shear regimes.

This trend is supported by the relatively higher n values (closer to unity) compared to XG and HPAM (Table 2), indicating reduced shear sensitivity and a more stable flow response under varying conditions.

The rheological behavior of FLOPAAM is consistent with the presence of sulfonate ($–SO_3^-$) functional groups, which are known to promote electrostatic stabilization and mitigate polymer chain contraction in electrolyte-containing media. Although the present study was conducted under diluted brine conditions (10% SB), the observed viscosity stability with temperature and shear rate aligns with the electrolyte tolerance widely reported for sulfonated polyacrylamides. These characteristics suggest that FLOPAAM may offer improved robustness under more saline reservoir environments.

3.4 Rheological Modeling Using the Ostwald–de Waele Power Law

The rheological behavior of xanthan gum (XG), partially hydrolyzed polyacrylamide (HPAM), and sulfonated polyacrylamide (FLOPAAM) solutions prepared in 10% synthetic brine was analyzed using the Ostwald–de Waele power-law model, a widely accepted framework for describing non-Newtonian (pseudoplastic) flow in polymer flooding applications. The model expresses apparent viscosity and shear stress as functions of shear rate according to the following equations:

$$\eta_{app} = K\dot{\gamma}^{n-1} \quad (1a)$$

$$\tau = K\dot{\gamma}^{n} \quad (1b)$$

where η_{app} is the apparent viscosity (Pa·s), τ is the shear stress (Pa), K is the consistency index ($Pa.s^n$), $\dot{\gamma}$ is the shear rate (s^{-1}), and n is the flow behavior index (dimensionless). The value of n characterizes the flow regime, with n =1 corresponding to Newtonian behavior, n >1 to shear-thickening behavior, and n <1 to shear-thinning behavior (Barnes, 1989). Equations (1a) and (1b) are mathematically related, as expressed in Eq. (1c).

$$\eta_{app} = \frac{\tau}{\dot{\gamma}} \quad (1c)$$

All experimental datasets exhibited values of n < 1, confirming the pseudoplastic nature of the evaluated polymer solutions under reservoir-representative temperature and pressure conditions. The fitted parameters summarized in Table 2 show excellent agreement between experimental data and the power-law model, with coefficients of determination exceeding 0.95 in all cases and typically higher than 0.98. These results confirm the suitability of the Ostwald–de Waele formulation for describing the shear-dependent rheological response within the investigated shear -rate range (1-100 s^{-1}), where no clear Newtonian plateau was observed.

Although more complex rheological models, such as the Carreau–Yasuda or Cross equations, can describe transitional regimes between Newtonian plateaus and shear-thinning regions, their multiparametric structure often requires extensive datasets and may introduce overparameterization, particularly when incorporating coupled temperature and pressure effects. In the present study, no clear Newtonian plateaus were experimentally observed within the investigated shear-rate range (1–100 s^{-1}).

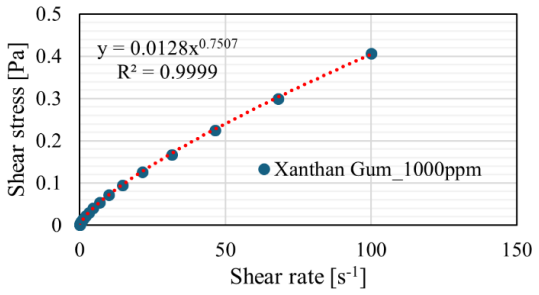

Fig. 5 Ostwald–de Waele model fitting for XG at 1000 ppm in 10% synthetic brine.

Under these conditions, the additional fitting parameters required by Carreau–Yasuda or Cross formulations would not provide substantial physical or predictive advantages over the Ostwald–de Waele model.

For this reason, the Ostwald–de Waele model was selected as a robust and computationally efficient framework, providing high fitting accuracy within the investigated experimental conditions while preserving the physical interpretability of the rheological parameters. This choice prioritizes model robustness and practical applicability over formulation novelty, which is particularly relevant for reservoir-scale implementation and polymer flooding design. These characteristics make it especially suitable for comparative analyses and for implementation in numerical reservoir simulators used in polymer flooding design.

At 80 °C, the consistency index K decreased systematically with decreasing polymer concentration, reflecting progressive weakening of the polymeric network under saline conditions. Among the evaluated systems, XG exhibited consistently high K values—particularly at intermediate concentrations— while HPAM showed the highest K values at the highest polymer concentrations. FLOPAAM showed lower K values but flow behavior indices closer to unity, suggesting reduced sensitivity to shear.

Figure 5 illustrates the excellent agreement between experimental data and the Ostwald–de Waele model for XG at 1000 ppm in 10% synthetic brine, demonstrating the ability of the power-law formulation to accurately capture the shear-thinning response across the investigated shear-rate range.

In this work, the Ostwald–de Waele model serves as the base rheological framework, upon which the effects of polymer concentration and temperature are incorporated through the consistency index $K(C,T)$ while the flow behavior index $n(C,T)$ is determined directly from experimental measurements. Pressure effects are addressed separately by applying a Barus-type formulation to the apparent viscosity at a reference shear rate, as discussed in subsequent sections. This hierarchical modeling strategy avoids overparameterization while ensuring physical consistency when extending the model to combined reservoir conditions.

3.5 *Analysis of the Concentration Effect and Rheological Modeling*

To evaluate the effect of polymer concentration on apparent viscosity under constant shear conditions, the experimental data presented in Figures 2–4 were analyzed. The analysis focused on the concentration-dependent evolution of apparent viscosity and its representation through the consistency index K of the Ostwald–de Waele model.

Figure 6A shows the variation of apparent viscosity for xanthan gum (XG) solutions at 80 °C in 10% synthetic brine, evaluated at three representative shear rates: 4.64 s^{-1}, 10 s^{-1}, and 100 s^{-1}, over a concentration range of 1000–5000 ppm. In all cases, apparent viscosity increased markedly with polymer concentration, with the effect being significantly more pronounced at low shear rates. At 4.64 s^{-1}, apparent viscosity values exceeded 540 mPa·s at 5000 ppm, reflecting the formation of dense and interconnected polymer networks that enhance flow resistance and structural integrity.

At higher shear rates (100 s^{-1}), apparent viscosity decreased substantially and exhibited a weaker dependence on concentration. This behavior is attributed to shear-induced alignment and partial disruption of the polymeric structure, which limits the contribution of intermolecular interactions to flow resistance. The observed shear-rate-dependent sensitivity to concentration is characteristic of pseudoplastic polymer solutions and is consistent with previous reports for polymer systems used in EOR applications. (Firozjaii *et al.*, 2020; Kumar *et al.*, 2025)

The effect of concentration is quantitatively captured by the consistency index K, obtained from the Ostwald–de Waele model fits. As shown in Figure 6B, K increases strongly and non-linearly with polymer concentration at constant temperature, indicating progressive strengthening of the polymeric structure as chain density and intermolecular interactions increase. Rather than a simple exponential dependence, the relationship between K and concentration follows a power-law–type behavior, which provides a more physically consistent description of polymer network development in saline media.

The systematic concentration dependence of K forms the basis for the extended rheological model developed in this work, where K is expressed as a function of both concentration and temperature, while the flow behavior index n is determined experimentally for each condition. By incorporating

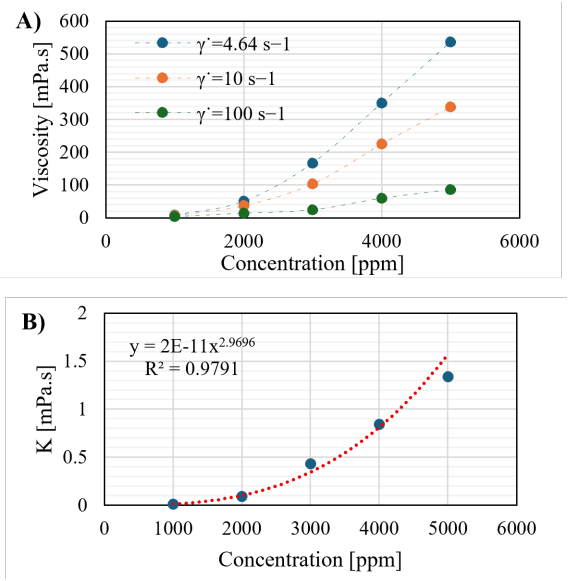

Fig. 6 (A) Apparent viscosity as a function of polymer concentration at different shear rates. (B) Consistency index (K) as a function of concentration for xanthan gum (XG) solution at 80 °C in 10% synthetic brine.

concentration effects through K (C,T), the model preserves physical interpretability and avoids overparameterization, enabling reliable prediction of apparent viscosity under reservoir-representative salinity and thermal conditions.

The strong agreement between experimental trends and the proposed concentration-dependent framework supports its suitability for describing polymer flooding rheology. Similar non-linear concentration effects on consistency index and apparent viscosity have been reported in the literature for polymer solutions in saline systems (Barnes, 1989; de Sá Costa *et al.*, 2013; Puente Córdova *et al.*, 2022). Consequently, the proposed approach provides a robust basis for optimizing polymer concentration in mobility-control applications and for supporting the rational design of Enhanced Oil Recovery (EOR) operations.

3.6 *Analysis of the Temperature Effect and Rheological Modeling*

To analyze the temperature effect on the rheological behavior of polymer solutions, isothermal rheological tests were conducted at a fixed polymer concentration, while temperature was varied from 20 to 80 °C. Apparent viscosity was measured over a wide range of shear rates to capture both low- and high-deformation regimes.

The experimental results (Figure 7A) show that increasing temperature leads to a systematic decrease in apparent viscosity at all evaluated shear rates. This effect is more pronounced at low shear rates (4.64 s^{-1}), where intermolecular interactions and

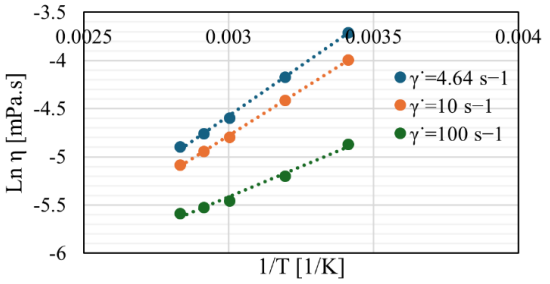

Fig. 7. Apparent viscosity as a function of temperature at different shear rates for xanthan gum (XG) solution.

Table 3. Ostwald–de Waele model parameters for xanthan gum (XG) at 1000 ppm in 10% synthetic brine.

Temperature (°C)	K (mPa.s^n)	n	R^2
80	0.006	0.7683	0.9977
70	0.0118	0.7507	0.9999
60	0.0148	0.74	0.9997
40	0.0219	0.7289	0.9979
20	0.0354	0.7141	0.9959

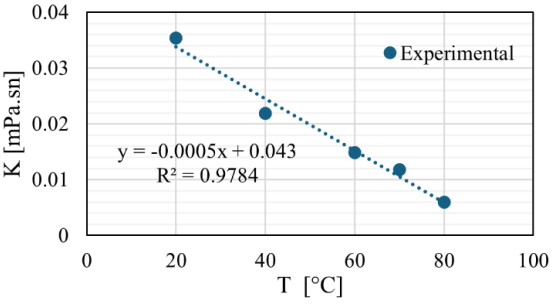

Fig. 8 Linear relationship between the consistency index (K) and temperature for xanthan gum (XG) solutions in 10% synthetic brine.

structural coherence dominate the flow response. As temperature increases, enhanced molecular mobility weakens intermolecular associations, facilitating chain rearrangement and flow.

The thermal sensitivity of the rheological response is also reflected in the variation of the flow behavior index n. As summarized in Table 3, n increases slightly with temperature, indicating a gradual transition toward less pseudoplastic behavior. This trend is associated with partial disruption of the polymeric network at elevated temperatures and has been widely reported for dilute and semi-dilute polymer solutions.

As shown in Figure 8, a nearly linear relationship between K and temperature was obtained for XG solutions in 10 % synthetic within the investigated temperature range (20–80 °C). This behavior was first described empirically by a linear relation (K =

$A_2 + B_2T$) and subsequently generalized through a separable Arrhenius-type formulation to account for the combined effects of polymer concentration and temperature. The resulting correlation is given by Equation (2):

$$In\ K(C,T) = a + b\ In\ \left(C_{Kppm}\right) + \frac{c}{T} \qquad (2)$$

where $C_{kppm}$is the polymer concentration expressed in kppm, T is the absolute temperature (K) and a, b, and c are fitted parameters. The flow behavior index $n(C,T)$was determined experimentally for each condition and was not further correlated to avoid overparameterization.

Although the present study was conducted under diluted brine conditions (10% SB), an increase in salinity toward the original reservoir value (~67,000 ppm) would be expected to modify the rheological parameters, particularly for salinity-sensitive polymers. In general, higher ionic strength would likely decrease the consistency index K due to enhanced electrostatic screening, polymer chain contraction, and reduced hydrodynamic volume, which would weaken intermolecular interactions and structural network strength. At the same time, the flow behavior index n may shift toward values closer to unity, indicating a less pronounced shear-thinning response. This effect would likely be more significant for HPAM, moderate for XG, and less pronounced for FLOPAAM due to the stabilizing effect of sulfonate groups under saline conditions.

3.7 Apparent viscosity Curves at High Pressure

The apparent viscosity–shear rate curves obtained at pressures up to 6000 psi confirmed the characteristic shear-thinning behavior of the three evaluated polymers—XG, HPAM, and FLOPAAM—under high-pressure conditions. In all cases, apparent viscosity decreased with increasing shear rate, reflecting progressive alignment and partial disruption of the polymeric structure under accelerated laminar flow, as illustrated in Figure 9.

Under high-pressure conditions, FLOPAAM exhibited the highest apparent viscosity values, particularly at low shear rates. At a shear rate of approximately 4.6 s^{-1}, viscosity values were on the order of 10^3 mPa·s for the 5000 ppm solution. This behavior suggests enhanced structural stability of the polymer network under combined pressure and thermal effects, consistent with the molecular architecture of sulfonated polyacrylamides, whose functional groups are known to improve conformational stability and resistance to chain contraction.

High-pressure measurements revealed a systematic decrease in apparent viscosity with increasing pressure for all evaluated polymers. This inverse pressure dependence may be attributed to compressive effects, including partial contraction of polymer coils and reduction of hydrodynamic volume. The magnitude of viscosity reduction was polymer dependent, being most pronounced for HPAM and least significant for FLOPAAM, suggesting superior resistance of sulfonated polyacrylamide networks to compressive deformation.

The effect of pressure on apparent viscosity was analyzed using a Barus-type exponential relation applied to the apparent viscosity at a reference shear rate rather than directly to the consistency index. This approach isolates the pressure contribution while preserving the structure of the power-law rheological model. The pressure dependence is expressed as Equation (3):

$$\eta_{app,10}(P) = \eta_{app,10}(P_{ref})exp[\alpha(P - P_{ref})] \qquad (3)$$

where $\eta_{app,10}$ is the apparent viscosity evaluated at $\dot{\gamma}$=10 s^{-1}, P is the pressure, P_{ref} is a reference pressure, and α is the pressure sensitivity coefficient. Negative values of α were obtained, indicating an inverse Barus-type pressure dependence. This behavior reflects pressure-induced structural contraction and reduced hydrodynamic volume.

In contrast to simple Newtonian liquids, where viscosity typically increases with pressure due to reduced free volume and restricted molecular mobility, polymer solutions exhibit a more complex response governed by macromolecular structure.

In the present systems, the observed decrease in apparent viscosity with increasing pressure can be attributed to pressure-induced conformational changes in polymer chains, including partial coil contraction and a reduction in effective hydrodynamic volume. Previous studies have reported that reductions in polymer coil dimensions and hydrodynamic volume can contribute to decreases in concentrated polymer systems subjected to externally induced compressive or interaction-driven stresses (Dunstan, 2019; Dunstan and Harvie, 2020). Under the investigated conditions, these macromolecular effects appear to dominate over the free-volume reduction effects typically responsible for pressure-induced viscosity increases in simple liquids.

This structural compression weakens intermolecular interactions and reduces network connectivity, particularly under conditions where the rheological response is dominated by chain entanglement and supramolecular organization. As a result, the effective resistance to flow decreases with increasing pressure, leading to the observed inverse Barus-type behavior. This effect is polymer-dependent and reflects differences in molecular architecture and functional groups, which influence the resistance of the polymer network to compressive deformation.

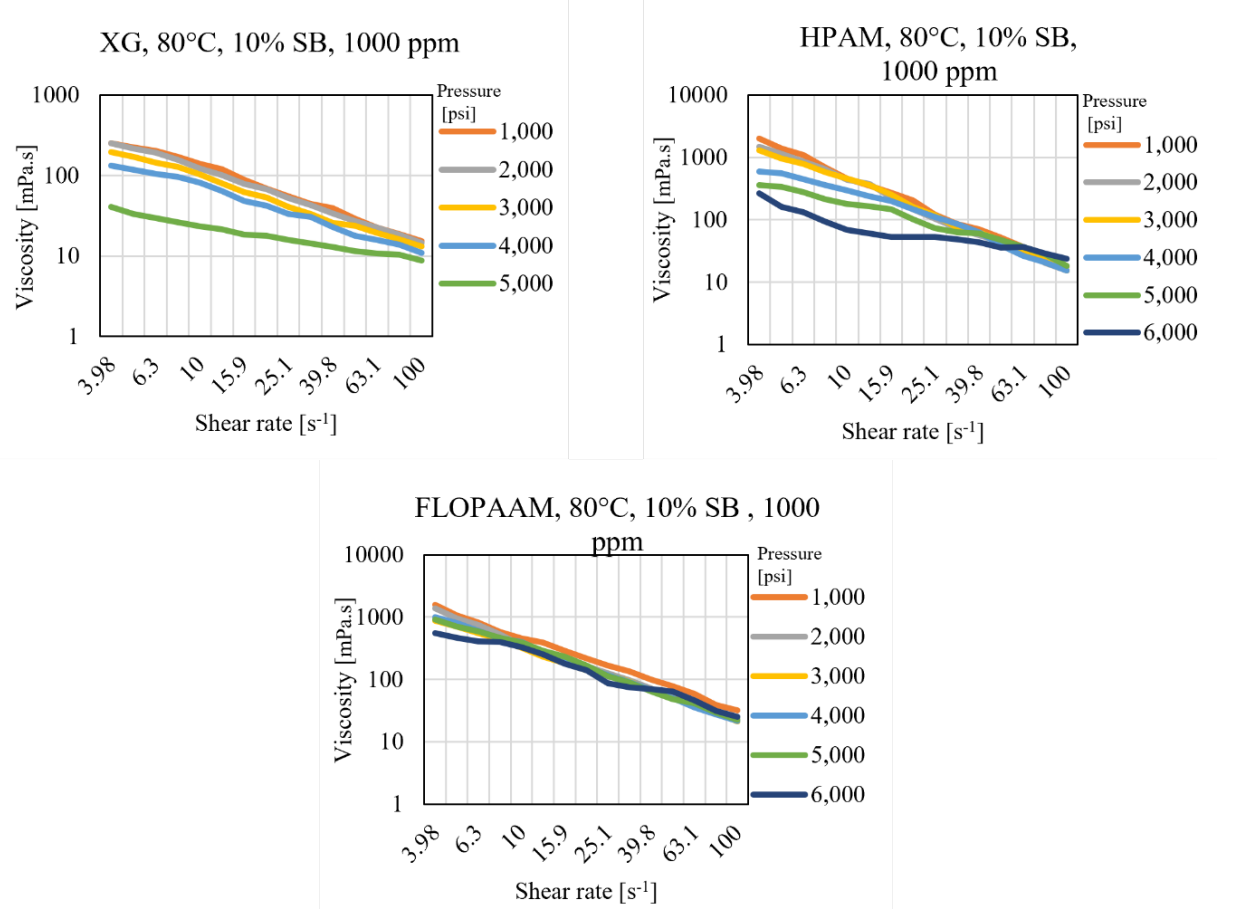

Fig. 9 Apparent viscosity–shear rate curves for XG, HPAM, and FLOPAAM solutions at 80°C and 1000ppm in 10% synthetic brine under different pressures (1000–6000 psi).

Table 4. Variation of apparent viscosity as a function of pressure.

Pressure, psi	XG, 10% SB (mPa·s)	HPAM, 10% SB (mPa·s)	FLOPAAM, 10% SB (mPa·s)
6000	ND	551	266
5000	40.7	908	357
4000	133	997	600
3000	197	868	1290
2000	253	1380	1480
1000	350	1570	1990

ND: not determined due to experimental limitations.

From an applied Enhanced Oil Recovery (EOR) perspective, FLOPAAM emerges as a promising polymer for high-pressure environments, exhibiting superior rheological stability under the studied temperature, pressure, and brine conditions. XG remains a viable option for moderate operating conditions, while HPAM maintained acceptable rheological performance at elevated temperatures despite its higher pressure sensitivity. Consequently, optimal polymer selection should consider the specific pressure and temperature conditions, along with formulation and concentration optimization.

Although polymer solutions may exhibit pressure-induced viscosity enhancement under specific thermodynamic regimes, the experimental data obtained in this study (Table 4) indicate a clear overall decrease in apparent viscosity with increasing pressure. This behavior suggests that compressive deformation and partial contraction of polymer coils dominate over free-volume reduction effects under the investigated conditions.

3.8 High-Pressure Rheological Modeling

The combined effect of high-pressure conditions on the rheological behavior of polymeric solutions was

Table 5. Fitted parameters of the Barus-type pressure–viscosity model for polymer solutions at 80 °C and 1000 ppm in 10% synthetic brine.

Polymer Solution	η_o (mPa·s)	α (psi^{-1})	R^2
XG–10% SB	583.29	-0.000427	0.9668
HPAM–10% SB	1807.2	-0.0002	0.9112
FLOPAAM–10% SB	3051.4	-0.0004	0.9516

evaluated, as pressure represents a critical operational parameter in reservoir applications. Experiments were conducted at a fixed salinity of 10% synthetic brine and a constant polymer concentration of 1000 ppm, while varying pressure at controlled temperatures and shear rates representative of reservoir flow conditions.

The experimental results summarized in Table 4 show a clear overall decrease in apparent viscosity with increasing pressure for XG, HPAM and FLOPAAM solutions. This inverse pressure dependence reflects the compressibility of the polymeric system and the sensitivity of the polymer network to confinement effects. At lower pressures, polymer chains experience reduced compressive stress, allowing partial network expansion and enhanced resistance to flow. Conversely, increasing pressure promotes structural compaction, leading to a reduction in the effective hydrodynamic volume and, consequently, lower apparent viscosity.

To quantify the pressure sensitivity of the polymeric solutions, the Barus-type exponential relation previously defined in Equation (3) was applied to the apparent viscosity evaluated at a reference shear rate. The fitted parameters obtained from this relation are reported in Table 5. For all evaluated polymers, negative values of α were obtained, indicating that apparent viscosity decreases with increasing pressure. This inverse Barus-type behavior is physically consistent with compressive deformation and partial contraction of the polymeric network under confinement. Unlike simple Newtonian fluids, where positive α values are often associated with pressure-induced viscosity enhancement, non-Newtonian polymeric systems may exhibit the opposite trend when pressure-driven structural effects dominate.

The magnitude of the pressure sensitivity coefficient (α) was polymer dependent. XG exhibited the largest absolute α values, indicating the strongest viscosity reduction with increasing pressure. In contrast, FLOPAAM showed lower pressure sensitivity, reflecting greater resistance of its polymeric network to compressive effects. HPAM displayed intermediate behavior. These differences confirm that polymer chemistry and chain architecture govern the mechanical stability of polymer solutions under confinement. Additionally, the pressure effect was more pronounced at low shear rates, where polymer-network contributions dominate the flow response.

Despite minor deviations at extreme pressures, the high coefficients of determination ($R^2 > 0.91$) demonstrate that the inverse Barus-type formulation provides a satisfactory quantitative description of the pressure dependence of apparent viscosity under reservoir-relevant conditions. These correlations enable reliable comparison of polymer performance under confinement and provide essential parameters for predicting rheological behavior during Enhanced Oil Recovery (EOR) operations at high pressure.

It should be noted that the pressure dependence was evaluated at a reference shear rate, which implies an assumption of separability between shear rate and pressure effects. This assumption represents a practical approximation that enables independent characterization of pressure sensitivity; however, it may not fully capture potential shear–pressure coupling effects in non-Newtonian polymer solutions.

The magnitude of viscosity reduction with pressure is quantitatively captured by the pressure sensitivity coefficient (α), which varies among the polymers (Table 5), confirming that FLOPAAM exhibits lower pressure sensitivity compared to XG and HPAM.

3.9 Extended Apparent viscosity Model as a Function of Temperature and Pressure

To integrate the combined effects of concentration, temperature, pressure, and shear rate on the rheological behavior of the polymeric solutions, a hierarchical and physically consistent framework was constructed based on the Ostwald–de Waele power-law model and the combination of established rheological correlations. In this approach, shear-rate dependence is described by the power-law formulation, while temperature and concentration effects are incorporated through the consistency index, and pressure effects are introduced independently via a Barus-type relation applied to a reference apparent viscosity.

Within this framework, the pressure contribution is treated independently from shear-rate effects. While this approach simplifies formulation and avoids overparameterization, it inherently assumes separability between shear rate and pressure, which may not be strictly valid under all conditions. Therefore, the proposed formulation should be

interpreted as an approximation suitable for the investigated experimental domain.

The apparent viscosity under combined operating conditions is expressed by Eq. (4):

$$\eta_{app}(C,T,P,\dot{\gamma}) = K(C,T)\dot{\gamma}^{n(C,T)-1} exp[\alpha(P - P_{ref})] \quad (4)$$

where: $\eta_{app}(C,T,P,\dot{\gamma})$ is the apparent viscosity (mPa·s), $\dot{\gamma}$ is the shear rate (s^{-1}), $K(C,T)$ is the consistency index incorporating concentration and temperature effects, $n(C,T)$ is the experimentally determined flow behavior index, P is pressure, P_{ref} is a reference pressure, and α is the pressure sensitivity coefficient obtained from high-pressure rheological measurements.

The temperature and concentration dependence of the consistency index was incorporated through the Arrhenius-type relation previously defined (Equation 2). Pressure effects were described using an inverse Barus-type formulation, reflecting compressive deformation and partial contraction of polymer coils under confinement. Negative α values indicate a decrease in apparent viscosity with increasing pressure, consistent with the experimentally observed behavior of non-Newtonian polymer solutions under high-pressure conditions. The parameter α may exhibit moderate dependence on temperature and local operating conditions.

As an illustrative example, for the xanthan gum (XG) solution at a concentration of 1000 ppm and a shear rate of approximately 4 s^{-1}, using a reference condition of T_{ref}=60°C (333.15 K) and P_{ref}=1000 psi, the resulting formulation enables the estimation of apparent viscosity as a function of temperature and pressure using the fitted parameters c=1705 K and α = - 4.27× 10^{-4} psi^{-1}.

Additionally, the interpolation capability of the proposed framework was evaluated through interpolation-based validation analyses for both temperature- and pressure-dependent behavior. HPAM was selected as a representative validation system due to its pronounced sensitivity to both temperature and pressure variations, providing a stringent test for the proposed framework.

For temperature dependence, the apparent viscosity of HPAM at 70 °C, 1000 ppm, and a shear rate of 10 s^{-1} was predicted using parameters obtained from data at 20, 40, 60, and 80 °C. The predicted viscosity (11.6 mPa·s) showed good agreement with the experimental value (12.0 mPa·s), with a relative error of approximately 3.3%.

For pressure dependence, the apparent viscosity of HPAM at 60 °C and 1000 ppm at 3000 psi was predicted using data from 1000, 2000, 4000, 5000, and 6000 psi. The predicted viscosity (399 mPa·s) showed excellent agreement with the experimental value (403 mPa·s), with a relative error of approximately 1%.

These results support the consistency of the proposed framework and demonstrate its interpolation capability for both temperature- and pressure-dependent behavior within the investigated experimental domain.

It is important to emphasize that the present formulation does not attempt to resolve the full coupling between shear rate and pressure, which would require a significantly more complex constitutive description and a substantially larger experimental dataset. Instead, the proposed framework adopts a separable representation as a physically motivated and application-oriented approximation, enabling robust parameter estimation and practical implementation under reservoir-representative conditions.

Within this context, the framework should be interpreted as a reduced-order description valid within the investigated parameter domain, rather than as a complete constitutive model capable of capturing all coupled rheological effects or providing universal predictive capability.

This formulation provides a continuous and physically consistent surface for interpolating apparent viscosity within the experimental domain investigated under combined reservoir-representative conditions. It enables reliable interpolation across the evaluated temperature and pressure ranges; however, this validity is limited to the experimental conditions considered. External validation using independent datasets and field-scale conditions is required to further assess its general predictive capability.

The proposed framework should not be interpreted as a generalized predictive tool trained on independent datasets, but rather as a physically grounded formulation calibrated within the experimental domain.

Conclusions

The rheological behavior of xanthan gum (XG), partially hydrolyzed polyacrylamide (HPAM), and sulfonated polyacrylamide (FLOPAAM) was systematically evaluated under controlled conditions of shear rate, temperature, pressure, and diluted synthetic brine (10% SB). These parameters are critical for polymer flooding and mobility control in Enhanced Oil Recovery (EOR) applications. The results demonstrate that polymer performance is governed by the interplay between intrinsic polymer chemistry and operating conditions, highlighting the necessity of condition-specific polymer selection.

Xanthan gum (XG) exhibited high thermal stability and maintained functional apparent viscosity under the studied brine conditions, even at relatively low concentrations. Its pronounced shear-thinning

behavior and elevated consistency index values indicate the formation of a well-developed polymer network, making XG particularly suitable for applications where temperature effects are dominant.

HPAM showed greater sensitivity to pressure and temperature, reflecting stronger dependence on operating conditions. Nevertheless, acceptable performance was achieved at higher concentrations, supporting its application under moderate temperature and pressure conditions when polymer concentration is properly optimized.

FLOPAAM demonstrated enhanced rheological stability under combined shear, temperature, and pressure effects, exhibiting the highest apparent viscosity retention under high-pressure conditions among the evaluated polymers. This behavior is consistent with the molecular architecture of sulfonated polyacrylamides, which contributes to improved conformational stability under thermomechanical stress. Consequently, FLOPAAM emerges as a robust candidate for high-pressure EOR applications within the investigated brine conditions.

The experimental data were accurately described using the Ostwald–de Waele power-law model, confirming the pseudoplastic nature of all evaluated polymer solutions, with coefficients of determination typically exceeding 0.98. Based on this approach, an integrated apparent viscosity framework was established by combining the power-law formulation with temperature–concentration and pressure-dependent correlations. In this formulation, shear-rate dependence is captured by the power-law formulation, while temperature and concentration effects are incorporated through the consistency index and pressure effects are introduced independently via an inverse Barus-type relation. This hierarchical modeling strategy avoids overparameterization while preserving physical interpretability. The contribution of this work lies in the consistent integration of these dependencies under reservoir-representative conditions, enabling practical implementation.

Overall, this study provides a physically consistent framework for describing and interpolating polymer rheology under coupled thermomechanical conditions. The proposed framework supports rational polymer selection and formulation design for EOR operations by explicitly accounting for the combined effects of shear rate, temperature, concentration, and pressure, thereby contributing to the development of thermomechanically stable polymer systems tailored to specific operating environments.

The proposed framework should be interpreted as a reduced-order description valid within the investigated domain. Future work should focus on validating the proposed framework using independent datasets, extending its applicability to higher salinity conditions, and assessing its performance at field scale.

Acknowledgements

The authors gratefully acknowledge the financial support provided by the Instituto Mexicano del Petróleo (IMP) through Project D.72011 “Recuperación mejorada de aceite en sistemas carbonatados fracturados mediante un proceso híbrido de agua de baja salinidad y productos químicos”.

References

Barnes, H. A., Hutton J. F., & Walters. K. (1989). *An Introduction to Rheology* (Vol. 3). Editorial Elsevier Science, Amsterdam, The Netherlands.

Carmona-Pérez J.M., Díaz-Viera M.A., Serrano-Saldaña E., Carreón-Calderón B., Coronado M., Andersson M.P., (2026). A geochemical diagnostic tool for enhanced oil recovery in a low salinity waterflooding process in carbonates. *Revista Mexicana de Ingeniería Química,* 25 (1), Ener26700. https://doi.org/10.24275/rmiq/ Ener26700

Castro García, R. H., Llanos Gallo, S., Rodriguez Ardila, J. L., Quintero Pérez, H. I., Manrique Ventura, E. J., & Zapata Arango, J. F. (2020). Heavy Oil and High-Temperature Polymer EOR Applications. *CT&F - Ciencia, Tecnología y Futuro*, 10(2), 73–83. https://doi.org/10.29047/01225383.258

Chen, Q., Wang, Y., Lu, Z., & Feng, Y. (2013). Thermoviscosifying polymer used for enhanced oil recovery: rheological behaviors and core flooding test. *Polymer Bulletin*, 70(2), 391–401. https://doi.org/10.1007/s00289-012-0798-7

De Sá Costa, B., dos Reis Coimbra, J. S., Martins, M. A., Garcia-Rojas, E. E., Telis-Romero, J., & De Oliveira, E. B. (2013). Rheological Behavior of Binary Aqueous Solutions of Poly(ethylene glycol) of 1500 g·mol −1 as Affected by Temperature and Polymer Concentration. *Journal of Chemical & Engineering Data*, 58(4), 838–844. https://doi.org/10.1021/je300712j

Dunstan, D.E, (2019). The viscosity-radius relationship for concentrated polymer solutions Shear. *Sci Rep*., 9, 543. https://doi.org/10.1038/s41598-018-36596-6

Dunstan, D.E., Harvie, D.J.E., (2020). Shear Induced Interactions Cause Polymer Compression. *Sci*

Rep., 10, 5531. https://doi.org/10.1038/s41598-020-62297-0

Firozjaii A.M., Saghafi H.R.,(2020). Review on chemical enhanced oil recovery using polymer flooding: Fundamentals, experimental and numerical simulation. *Petroleum.* 6(2), 115-122. https://doi.org/10.1016/j.petlm.2019.09.003

Gbadamosi, A. O., Junin, R., Manan, M. A., Agi, A., & Yusuff, A. S. (2019). An overview of chemical enhanced oil recovery: recent advances and prospects. *International Nano Letters*, 9(3), 171–202. https://doi.org/10.1007/s40089-019-0272-8

Ghalamizade S.M., Saeedi A.H., Razavinezhad J., Tanhay R.,(2025), Effect of potential determining ions on sulfonated polyacrylamide behavior during smart water-polymer injection into carbonate reservoirs. *Petroleum*, 11(1), 41-55. https://doi.org/10.1016/j.petlm.2024.12.002

Gomaa S., Salem K.G., El-hoshoudy A.N., (2024). Enhanced heavy and extra heavy oil recovery: Current status and new trends. *Petroleum*, 10(3), 399-410. https://doi.org/10.1016/j.petlm.2023.10.001

Kumar G., Mahajan S., Agrawal A., Deshmukh M., Sangwai J., (2025). Enhanced Oil Recovery Using Viscosity-Augmented Guar Gum: A Comparative Study with Xanthan Gum and Partially Hydrolyzed Polyacrylamide. *Energy Fuels.* 39 (4), 1856–1869. https://doi.org/10.1021/acs.energyfuels.4c05116

Puente Córdova, J. G., Hernández Ramírez, C. L., Reyes Melo, M. E., Rentería Baltiérrez, F. Y., & Miranda Valdez, I. Y. (2022). Estudio reológico de soluciones poliméricas de carboximetil celulosa. *Ingeniería Investigación y Tecnología*, 23(2), 1–10. https://doi.org/10.22201/fi.25940732e.2022.23.2.012

Rock, A., Hincapie, R. E., Tahir, M., Langanke, N., & Ganzer, L. (2020). On the Role of Polymer Viscoelasticity in Enhanced Oil Recovery: Extensive Laboratory Data and Review. *Polymers*, 12(10), 2276. https://doi.org/10.3390/polym12102276

Saeed, M., & Jadhawar, P. (2023). Surface Complexation Modeling of HPAM Polymer–Brine–Sandstone Interfaces for Application in Low-Salinity Polymer Flooding. *Energy & Fuels*, 37(9), 6585–6600. https://doi.org/10.1021/acs.energyfuels.3c00542

Seright, R. S. (2017). How Much Polymer Should Be Injected During a Polymer Flood? Review of Previous and Current Practices. *SPE Journal*, 22(01), 1–18. https://doi.org/10.2118/179543-PA

Skauge, T., Ormehaug, P. A., Alsumaiti, A., Masalmeh, S., & Skauge, A. (2022). Polymer Stability at Harsh Temperature and Salinity Conditions. Paper Number: SPE-200178-MS. March 21-23. Muscat, Oman, *SPE Conference at Oman Petroleum & Energy Show.* https://doi.org/10.2118/200178-MS

Soto-Caballero M.C., Valdez-Fragoso A., Salinas-Lopez A.N.,Welti-Chanes J.,Verardo V., Mujica-Paz H., (2016). Rheological parameters of xanthan gum/pectin solutions as a function of temperature and composition. *Revista Mexicana de Ingeniería Química,* 15 (3), 859-868.

Tahir, M., Hincapie, R. E., & Ganzer, L. (2020). An Elongational and Shear Evaluation of Polymer Viscoelasticity during Flow in Porous Media. *Applied Sciences,* 10(12), 4152. https://doi.org/10.3390/app10124152

Tapias Hernandez, F. A., Lizcano Niño, J. C., & Zanoni Lopes Moreno., R. B. (2018). Effects of salts and temperature on rheological and viscoelastic behavior of low molecular weight HPAM solutions. *Revista Fuentes El Reventón Energético,* 16(1), 19–35. https://doi.org/10.18273/revfue.v16n1-2018002

Zaitoun, A., & Kohler, N. (1988). Two-Phase Flow Through Porous Media: Effect of an Adsorbed Polymer Layer. Paper Number: SPE-18085-MS. October 2-5. Houston, Texas, *SPE Annual Technical Conference and Exhibition.* https://doi.org/10.2118/18085-MS